Case Studies in Construction Materials 19 (2023) e02600

Contents lists available at ScienceDirect

Case Studies in Construction Materials

journal homepage: www.elsevier.com/locate/cscm

Performance-related methods for the characterization of cold mix patching materials used in asphalt pavements maintenance

Raheb Hafezzadeh [*,1], Federico Autelitano [2], Felice Giuliani [3]

Dipartimento di Ingegneria e Architettura, University of Parma, Parma, Italy

ARTICLE INFO

Keywords:
Cold mix asphalt
Pothole
Patch materials
Pavement maintenance
Localized distress

ABSTRACT

Cold mix patching materials (CMPMs) are commonly used as an alternative to hot mix asphalt (HMA) for repairing road pavement potholes, especially in cold and wet seasons. Currently, the acceptance criteria and expectations for the mechanical strength and durability of CMPMs are often compared or related to those adopted for traditional HMA pavements without considering the specific performance characteristics of CMPMs required to ensure their effectiveness. In response to this, the authors proposed innovative solutions derived from pre-existing methodologies to evaluate CMPMs. Several parameters, indicative of CMPMs' structural and functional performance, were measured to optimize the mix design and systematize the quality assurance/quality control (QA/QC) process at various service life stages and under different boundary conditions. Besides the standard Marshall stability and indirect tensile strength (ITS), which were chosen as references, Hubbard-Field and indentation stability tests were reintroduced, suggesting modified procedures specifically tailored to CMPM stability evaluation. Similarly, brush, Leutner, and locking point test methods were customized for analyzing the raveling potential, bonding properties, and workability of the patching materials. The research outcome showed that Hubbard-Field and indentation stability tests provided more accurate stability assessments, even for materials unsuitable for testing using Marshall stability and ITS methods. Modified brush and Leutner tests effectively replicated real-world conditions, enhancing the relevance of laboratory findings to practical applications. Furthermore, the locking point method enabled mixture workability classification. These findings contribute to a better understanding of CMPM performance and can inform more targeted and effective road repair strategies.

1. Introduction

Potholes are a prevalent form of asphalt pavement damage that often represents the final stage of one or more previously untreated failures. These localized depressions and breakdowns in the pavement surface occur due to material loss and can rapidly expand during the winter and spring seasons. They pose a significant risk to road users, compromising traffic safety and increasing the likelihood of accidents and injuries [1,2]. In recent years, cold mix patching materials (CMPMs) have gained popularity as an alternative to HMA for

* Correspondence to: Dipartimento di Ingegneria e Architettura, University of Parma, Parco Area delle Scienze, 181/A, 43124 Parma, Italy.
E-mail address: raheb.hafezzadeh@unipr.it (R. Hafezzadeh).
[1] ORCiD: https://orcid.org/0000-0002-8533-459X
[2] ORCiD: https://orcid.org/0000-0003-0780-9438
[3] ORCiD: https://orcid.org/0000-0002-8842-5083

https://doi.org/10.1016/j.cscm.2023.e02600
Received 12 April 2023; Received in revised form 13 September 2023; Accepted 20 October 2023
Available online 21 October 2023

repairing potholes and restoring road serviceability, especially in colder weather, thanks to their ease of handling, cost-effectiveness, low labor and equipment requirements, lower environmental impact, and longer storage time [3,4]. These ready-to-use patching materials typically consist of a blend of aggregates, binders, and additives. In their production, the binder is derived from virgin asphalt-based binders (in the form of asphalt emulsion, cutback, or proprietary binders) or obtained from either reclaimed asphalt pavement (RAP) or recycled asphalt shingle (RAS) [5–7]. CMPMs are easy and quick to apply; after opening the bag, they can be directly placed into a pothole and compacted using feet, a hand tamper, and a truck wheel [8]. The expected service life of most CMPMs, starting immediately after the repair operation and continuing until the complete patch deterioration, is about 3–12 months, which is highly dependent on the quality of material, application techniques, and the prevalent climate and loading conditions [9]. However, errors in the mix design, the use of poorly stored or expired materials, and incorrect application techniques or conditions are often associated with early defects and drawbacks [10]. After the reopening of traffic and in the first hours after patching operations, the patches have a high potential to face abrasion, rutting, shoving, and bonding issues. The severity of these distresses varies over time as the patches cure and compact under traffic flow [11,12].

In most scenarios, the failures of cold patching mixes are due to harsh weather conditions at the time of repair and improper construction techniques, mainly attributable to incorrect pothole preparation and insufficient material compaction. Practical laboratory-scale and on-field studies have shown that the workability of the CMPMs has the highest effect on compactability and, subsequently, patch survival [13]. Conversely, inadequate compaction leads to higher air-void content (up to 30%), becoming the primary cause of different in-service failures such as shoving, raveling, rutting, and dishing [14,15]. A tailored mix design is necessary to obtain a patching mixture capable of highlighting improved workability during placement, developing increased resistance to early traffic, and maintaining good adhesion and mechanical strength throughout the service life. Manufacturers are used to adjusting the mix design based on the season, differentiating between spring, fall, and winter applications to ensure optimal performance. The materials can show different behavior in various seasonal conditions. Well-designed and correctly applied CMPMs can often outlast the surrounding pavement when applied on pavements affected by high-severity surface defects or distresses (e.g. cracking) [10,16]. When the material is poured and spread, it should be soft and pliable enough to be relatively easy to place and compact using common hand tools. Although several standards and test methods, such as dipping a spatula into the mixture [17], a cement concrete penetrometer (PTI method) [17,18], the blade resistance test [19], triaxial compression and unconfined compression tests [20], slump test [10], have been proposed in the previous studies to assess the workability of cold patching mixes, some of them do not necessarily distinguish different mixtures, identify poorly performing mixes, and show no strong correlation between laboratory and field results [10].

Mixtures with poor workability pose challenges during placement and compaction, significantly impacting the durability and stability of patches [10]. Immediately after opening to traffic, poorly compacted material could experience premature distress in the form of raveling and abrasion. Currently, the measurement of CMPMs raveling potential remains understudied in the scientific and commercial literature. Only a few studies that utilized the Cantabro test to investigate the raveling properties of cold mixtures were identified [11,21]. During the patch service life, the lack of stability can lead to dishing and shoving on the patches. A patching mixture should be stable after placement and compaction to resist vertical and horizontal displacement under traffic loads, particularly right after installation when the material is still uncured [22]. Stability is perhaps one of the few requirements often reported in product data sheets. Several test methods, such as resilient modulus, Marshall stability, indirect tensile strength [19], triaxial compression (confined and unconfined) [23], Hamburg wheel tracking [16], and penetration shear [24] tests, were recommended and employed by researchers to evaluate the stability of the CMPMs. However, these procedures are often derived from traditional HMA practices, and most of them have been designed to evaluate the performance of HMA. As a result, these tests were, in some cases, too severe for CMPMs, leading to questionable findings with poor correlation between laboratory and field results. Moreover, during the evaluation of CMPM stability, the established techniques often used oven-aged mixtures to ensure they were stable enough before conducting the tests [18]. However, the oven-aged samples may not accurately represent the material's behavior immediately after patching. Also, this approach may be problematic for testing water-reactive patching materials [15].

Additionally, potholes repaired during colder seasons tend to have a brief lifespan since the bonding between the patching material and the existing pavement is often insufficient. In some instances, the initial traffic flow can even dislodge these patched potholes [19]. Analyzing the bonding properties at the laboratory scale is a complex process that involves preparing composite specimens (half CMPM and half HMA) [25]. Researchers have conducted various studies aiming to evaluate factors such as the maximum shear force at the interface in different shear configurations [26] or the time required for debonding as a reference parameter [27]. However, these studies have produced conflicting results, making it challenging to derive comprehensive conclusions. Despite the limitations of these procedures in fully reflecting the bonding characteristics of CMPMs, they still serve a practical purpose in assessing the quality of cold patches [28].

In the light of the abovementioned, this article aimed to identify different test methods and approaches to evaluate the performance of CMPMs and to optimize the mix-design of these materials and systematized the quality assurance/quality control (QA/QC) procedures in their various service life stages. Thus, modified versions, adopted to the specific nature of CMPMs, of well-known methodologies in the road construction context as well as original procedures, have been considered to test unaged materials. To observe the performance and effectiveness of the recommended procedures and methods, three different types of patching materials, including solvent-containing mixtures (SC), membrane-containing mixtures (MC) and water-reactive mixtures (W*R*) were tested in the laboratory. The outcomes are anticipated to enhance awareness regarding the performance of CMPMs among patching material designers and material users under diverse weather and traffic conditions and enable manufacturers to improve the characteristics of their products through the availability of an experimental framework specific to the lifetimes of different pothole repair materials.

2. Selected materials

To assess the effectiveness of recommended methods and approaches in qualifying CMPMs, three commercially available products, belonging to each of the mentioned categories (SC, MC, and W*R*), were selected. Although each product uses a proprietary formulation, some distinctive characteristics can be pointed out. Specifically, the SC material is a mix of aged binder (recovered from RAP aggregates), aggregates (virgin plus RAP aggregates), and a blend of additives. This type of patching material is the cheapest and lowest-quality product used in the market, but it is widely purchased and used by road maintenance organizations due to its low price. In addition to virgin aggregates, RAP, and additives, the MC product also contains RAS in the mix design. The production and use of this kind of mixture, which offers a reasonable price and almost medium-to-high quality, have grown significantly in recent years. The W*R* product contains a special proprietary binder and a blend of additives that ensure rapid hardening of the mixture through a chemical reaction when exposed to water. This type of CMPM usually comes at a higher price than the other products but provides a high-quality patch. Due to the sensitivity of W*R* mixtures to moisture and their faster hardening when in contact with water, they are packed in sealed buckets.

The binder content (EN 12697–39), aggregate gradation (ASTM D6913–04), and the theoretical maximum density (ρm, as specified in EN 12697–5) of the mixtures have been presented in Table 1. The aggregate gradation in the mixtures used for this study adhered to the prescribed aggregate gradation for homemade cold patches, which is as follows: 9.5 mm (95–100%), 4.75 mm (40–85%), 2.36 mm (15–40%), 1.16 mm (6–25%), and 0.075 mm (1–6%) [29].

3. Methodology

After evaluating the binder content of the mixtures (according to EN 12697–39), aggregate gradation (as per ASTM D6913–04), and the theoretical maximum density (according to EN 12697–5), several methods and procedures (as shown in Fig. 1) were explored and set up to examine different physical-mechanical characteristics of the CMPMs. These tests, which include assessments of mix workability, stability, reveling and bonding, were performed at room temperature on specimens prepared using a Marshall hammer and a Superpave gyratory compactor (SGC).

3.1. Specimen preparation

Compaction CMPMs in patching potholes is a crucial step in the repair operation, which is usually performed manually by the road maintenance crew. Therefore, the resulting density can vary depending on the effort exerted by each person and the dimensions of the pothole. Cylindrical specimens with a diameter (D) of 100 mm and a nominal thickness of 65 ± 5 mm (thick) or 35 ± 5 mm (thin) were prepared using a Marshall hammer and an SGC. For compaction with the Marshall hammer, three sets of blows per side were employed, namely 35, 50, and 75. On the other hand, for gyratory compaction, pressures ranging from 200 to 600 kPa were selected, and the gyrations were set to 100 and 200. The compaction quantities (pressure and number of blows and gyrations) were selected each time based on the material characteristics and the performance test method. For each specimen, three replicates were prepared and the reported value for each test represents the mean of at least three independent measures.

Acronyms (e.g., WR_M75t) were used to label each mixture. The first pair of letters describe the material type (SC, MC, or W*R*), the letter after the underscore symbol defines the compaction procedure (M = Marshall hammer and G = Superpave Gyratory compactor), the numbers refer to the compaction effort (XX = the number of blows for Marshall Hammer; Y&Z = compaction pressure in kPa/100 and gyrations in number/100 for the Superpave Gyratory compactor), and the last letter identifies the specimen thickness (T = 65 mm; t = 30 mm). For example, the label WR_G2&1T denotes a specimen of the water-reactive material, which was compacted with the Superpave gyratory compactor at a pressure of 200 kPa for 100 gyrations, yielding a final thickness of 65 ± 5 mm. Similarly, SC_M50t signifies a solvent-containing sample compacted by 50 hammer blows using a Marshall hammer, resulting in a final thickness of 35 ± 5 mm.

3.2. Specimen storage

Researchers usually consider a preliminary aging process at higher temperatures in oven to enhance the stability of specimens and prevent them from collapsing after demolding when assessing the mechanical parameters of cold mixtures [15,30]. Nevertheless, these

Table 1
Aggregate gradation of the selected CMPMs.

	Sieve size [mm]									ρ_m	Binder content
	10.0	8.0	6.3	4.0	2.0	1.0	0.5	0.25	0.063		
	Cumulative passing [%]									[g/cm^3]	[%]
SC	99.8	99.7	95.3	50.0	19.3	12.0	9.1	7.9	6.4	2.57	4.78
MC	99.8	99.6	97.6	64.0	24.4	15.8	11.9	8.9	6.2	2.64	6.62
WR	100.0	99.0	91.8	64.6	36.6	20.2	11.1	7.4	3.4	2.41	6.71
Upper	100.0	95.5	88.5	71.2	36.1	22.7	13.7	9.5	6.0		
lower	96.0	78.4	58.7	32.3	12.1	5.2	2.9	1.8	1.0		

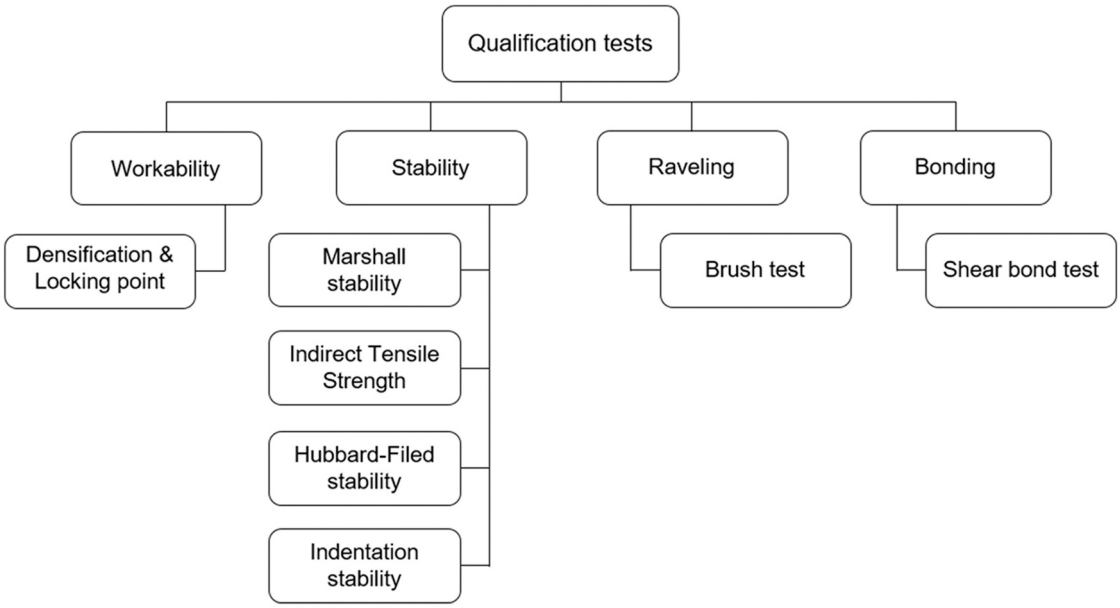

Fig. 1. Test methods and approaches to qualify CMPMs.

accelerated and artificial aging procedures may affect the behavior of the CMPMs, without offering a clear evaluation of the actual curing mechanisms following application and compaction. Thus, prior initiating testing, the unaged specimens were stored on a flat surface at laboratory conditions (temperature T = 22 ± 2 °C; relative humidity RH = 55 ± 5%) for up to 30 days from the time of their manufacture. Two different conditioning temperatures were generally considered for the specimens before testing, i.e., 20 and 60 °C with a tolerance of 2 °C.

3.3. Test methods

3.3.1. Densification and locking point

The density and locking point measured during the specimens' preparation phase were used to evaluate the compactability and workability of the mixtures. Two mixture conditioning temperatures were considered before compacting the samples, i.e., 2 ± 1 and 20 ± 1 °C, attributable to maintenance operations conducted in winter and spring. The CMPMs and the compaction mold (collar, cylinder, and plate) were preliminarily conditioned in a climate chamber for 24 h before making the specimens. After conditioning, the materials were compacted using the SGC and their densities and locking points were measured to evaluate their compactability. As, the compaction energy and the number of blows required to compact CMPMs and replicate the field densification are unknown, squared potholes with a size of 450 × 450 mm and a depth of 35 ± 5 mm were made on road pavement and filled with the CMPMs (T = 25 °C) and compacted using a hand tamper. A non-nuclear electromagnetic density gauge was used to measure the density of the patches in the field. Therefore, the densification of the lab and field can be compared and the equivalent required pressure to compact the mixtures in the lab can be determined.

The concept of the "locking point" was defined by Hemsley as the number of gyrations during material compaction with an SGC at which no noticeable changes in the thickness of the specimens are detected after three continuous gyrations [31]. Therefore, a workable material needs fewer gyrations or lower compaction energy to reach its locking point. In other words, a lower locking point indicates a more workable material and vice versa.

3.3.2. Stability

3.3.2.1. Marshall stability. The Marshall stability test was conducted following EN 12697–34 standard procedures to measure the resistance of specimens to plastic flow. The unaged mixtures were compacted using an SGC at 200 kPa for 100 gyrations. The prepared specimens were tested immediately after demolding, after 7, and 30 days of curing at room temperature. Before conducting the test, the specimens were conditioned (at 20 ± 1 °C and 60 ± 2 °C) for 30 min.

3.3.2.2. Indirect tensile strength. The specimens were fabricated using a method similar to the Marshall stability test and were subsequently conditioned at 20 ± 1 °C before testing. The experiments were conducted at the same temperature after undergoing up to 30 days of curing under laboratory conditions. The load was applied at a constant deformation rate of 50 mm/min to accurately determine the ITS of the specimens, adhering to the EN 12697–23 standard procedure.

3.3.2.3. Hubbard-Field stability. The Hubbard-Field method is an outdated procedure to determine the optimum asphalt content for a particular blend or gradation of aggregates [32]. A new modified version of this method was considered to evaluate the stability of the CMPM samples that were not stable enough after demolding. Contrary to the original method, the testing mold assembly was customized for our purpose, and cylindrical specimens with a diameter of 102 mm and a thickness of 25.4 mm were considered based on the mold size requirements. 380 g of CMPM were compacted using an SGC at 200 kPa for 35 gyrations (their locking point). The prepared specimens with a thickness of 25–30 mm were cured for up to 30 days in laboratory conditions, and they were conditioned in a water bath at 60 ± 2 °C for 30 min before conducting the test. Then, the prepared specimens were placed in the mold and squeezed through a plunger and a ring slightly smaller than the specimen diameter (Fig. 2). The peak load sustained before the mix started flowing through the orifice was recorded as the CMPM stability.

3.3.2.4. Indentation stability. The indentation test method (EN 12697–20 standard) is used to determine the depth of indentation of mastic asphalt and other asphalts (with aggregates having a maximum nominal size of 16 mm) when force is applied to specimens via a cylindrical indentor pin with a flat-ended circular base. The concept of this standard was used to evaluate the stability of CMPMs. Since the patch is surrounded by the edges of the pothole, in addition to the mold-free specimens, mold-surrounded specimens were also considered. The mixtures were compacted by an SGC at 200 kPa for 100 gyrations and cured for 24 h in laboratory conditions (no water-bath conditioning). Then, the produced specimens were placed on a plate under the indentor pin with a circular flat-ended bas (ϕ =25.2 mm), and static weights of 53 kg were applied through the flat-ended cylinder at 25 ± 1 °C (Fig. 3). The indentation depth of the cylinder over time was recorded and reported as a measure of CMPM stability.

3.3.3. Raveling

Raveling is typically caused by a loss of bonding between aggregates and binders, as well as mechanical dislodging from certain types of traffic, such as snowplow blades or tracked vehicle [29,30]. So, the authors proposed a modified version of the brush test (EN 12697–43) to evaluate the raveling characteristics of CMPMs, which can better simulate the abrasion and raveling of the cold patches in the lab. Through this modified test procedure, the specimens were compacted using an SGC for 100 gyrations at 200, 400, and 600 kPa of pressure. This pressure range was selected to consider the field compaction, which varies from poor to excellent depending on the effort used by the crew. A Hobart mixer with a circle mold attached to its bottom side was used to perform the test (Fig. 3). The specimens (t = 65 ± 5 mm) were mounted on the mold, while an air pressure of 150 kPa (1.5 bar) was applied to the bottom of the mold to lift the system of the mold and specimen. Less than 150 kPa was not able to lift the samples. At higher pressures, the specimens were compressed between the wire brush and the mold, resulting in abnormal weight loss. After applying the air, the specimen comes into contact with the 60 rpm rotating wire brush. Then, the mass loss was calculated after 30, 60, and 120 s

3.3.4. Bonding

The shear bond test (EN 12697–48), also known as the Leutner test, was considered to determine the interface shear bond between two asphalt layers. To assess the bonding between the cold patch and existing layer, 600 g of the CMPM were compacted onto a reference dense-graded HMA specimen using an SGC at a pressure of 200 kPa for 100 gyrations (Fig. 4-a). The resulting thickness of the compacted CMPM layer was 35–40 mm, which is equal to the depth of a medium-sized pothole. The prepared specimens were

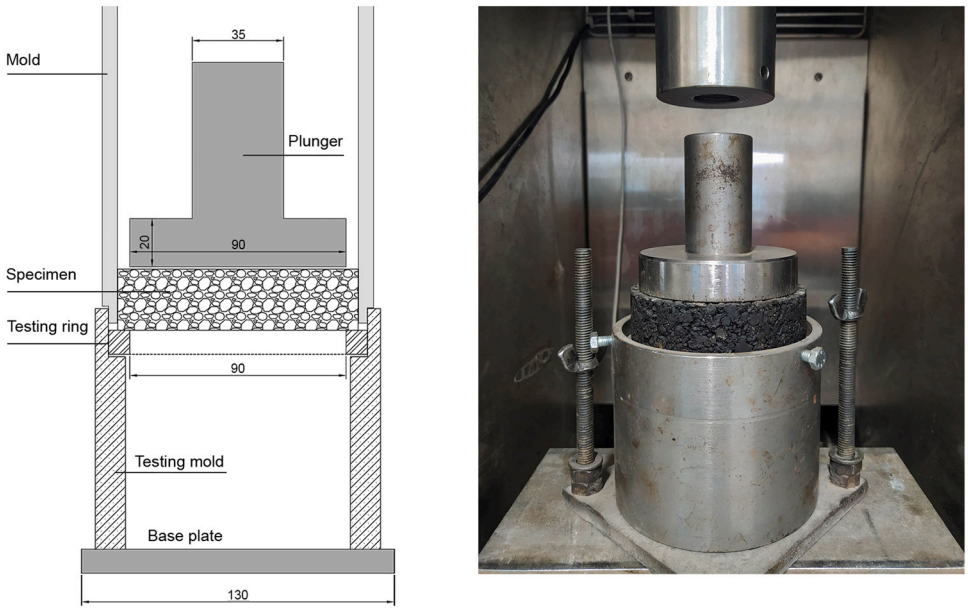

Fig. 2. Hubbard-Field stability test (the dimensions in the scheme are based on mm).

Fig. 3. Indentation test device. Utilizing brush test to assess the raveling potential of CMPMs.

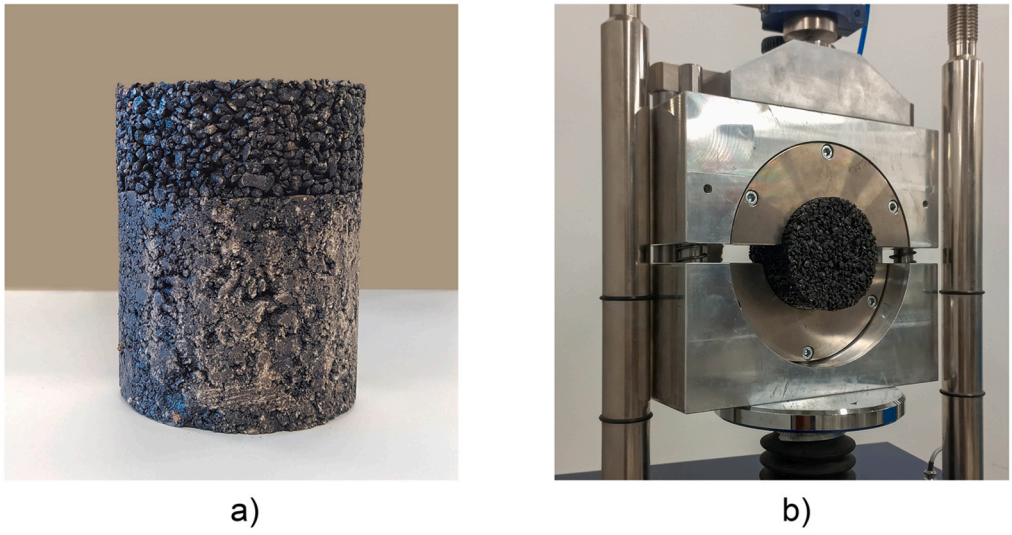

Fig. 4. Interlayer shear bond test: a) Composite specimen b) Leutner head.

conditioned at 20 ± 1 °C for 24 h before performing the test. Then, they were placed on Leutner's head to conduct the test (Fig. 4-b). Due to the poor initial bonding characteristics of CMPMs, the load was applied to the specimen at a rate of 2.5 mm per minute rather than 50 mm per minute. When the shear force dropped to 70% of the maximum shear force, the test was stopped, and the recorded shear force (F) versus the displacement (δ) was plotted (Fig. 5) to calculate the required parameters, such as shear energy (the area under the shear force-displacement graph) and the slope of the line graph (the linear part of the graph in Fig. 5). Then, the maximum shear stress at the interface ($\tau_{SBT,\max}$and the interface shear stiffness modulus ($K_{SBT,\max}$)are calculated according to Eqs. 1 and 2.

$$\tau_{SBT,\max} = \frac{F_{SBT,\max}}{\left(\frac{D}{2}\right)^2}.1000 \quad [\text{MPa}] \tag{1}$$

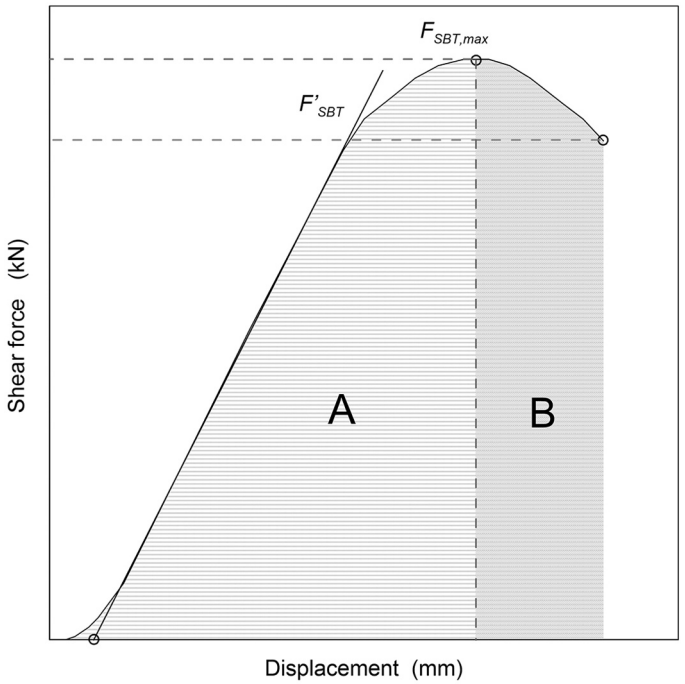

Fig. 5. The shear force vs. the displacement obtained from the shear bond test.

$$K_{SBT,\max} = \frac{F'_{SBT}}{\pi \bullet \left(\frac{D}{2}\right)^2} \quad [\mathrm{MPa/mm}] \tag{2}$$

where $F_{SBT,\max}$ is the maximum vertical shear force (kN), D is the initial diameter of the specimen in the interlayer (mm) and F'_{SBT} is the slope of the linear part of the force-displacement graph (kN/mm). The shear energy ($Eng_{,i}$) is expressed by dividing the area under the shear force-displacement curve (the work of failure) by the cross-sectional area of the specimen.

4. Results and discussion

4.1. Densification and locking point

The densification and air-void results obtained from the field patches and laboratory thick and thin specimens were presented in Table 2. As it can be seen, when the SGC was used to compact the mixtures, the thicker specimens (65 ± 5 mm) led to lower air-void contents compared to thinner specimens. However, depending on the workability and compactability of the CMPMs, thin specimens (35 ± 5 mm) compacted by the Marshall hammer led to better or worse densification than SGC. Therefore, the depth of the pothole, the thickness of the specimen, and the characteristics of the material can help to select the proper compaction method or device in the laboratory to replicate field compaction. The air-void (density) contents obtained from the field patches were comparable to those

Table 2
Air-void content achieved from laboratory specimens and field patches at 20 °C.

	Laboratory										Field
Thickness	T: 65 ± 5 mm (Thick)					t: 35 ± 5 mm (Thin)					
Compaction Method	S2&2	S6&2	M35	M50	M75	S2&2	S6&2	M35	M50	M75	Hand tamper
Material	Air void content [%]										
SC	26.03	20.97	27.04	25.07	24.38	*	24.66	26.17	24.38	21.1	22.3
MC	29.18	22.56	33.03	30.18	28.53	*	23.95	29.52	28.55	26.3	20.5
WR	13.69	9.73	13.4	12.2	10.68	*	10.7	12.1	11.5	11.0	13.8

* There is no data

obtained from lab (thick or thin) specimens, considering 75 blows of the Marshall hammer or 600 kPa SGC for 200 gyrations. Thus, to replicate the field compaction great compaction pressure is required in the laboratory. By way of example, Fig. 6 depicts in more detail the impact of the compaction pressure on the density (ratio of bulk specific gravity to theoretical maximum specific gravity) of the MC mixture. According to the graphs, the increase in compaction pressure decreased the air void contents. This influence is much more noticeable when a pothole is deep, and the patching materials need to be compacted well with more effort by the crew to provide a denser patch. Poor compaction leads to higher air void contents and increases the potential for patch failure in a short time. This trend is much more remarkable when mixtures are compacted by an SGC than by a Marshall hammer, as air void contents have higher differences between mixtures compacted with an SGC at the same number of gyrations but different compaction pressures. This difference is lower for mixtures compacted with a Marshall hammer at the same number of blows. For example, the air void content difference between mixtures that were compacted using a Marshall hammer at 35 and 75 was not as great as the air void differences between mixtures compacted by an SGC at 200 and 600 kPa at each gyration.

Focusing on the impact of compaction pressure, Fig. 7 displays the thickness versus air void content of specimens compacted with 35, 50, and 75 blows per side. As expected, at each set of hammer blows, the workable mixture resulted in thinner specimens, indicating lower air void content. W*R* and MC cold mixtures highlighted the highest and lowest thickness reduction at each set of blows, which implies that W*R* and MC had the best and worst compactability, respectively. In other words, considering the equal number of hammer blows for compacting the CMPMs, the W*R* and MC mixtures were compacted better and worse than the others, as the achieved thickness and, subsequently, their air-void content were the lowest and highest, respectively. Although the thickness or air void content of the specimens (resulting from compaction energy) was beneficial for comparing the compactability of different CMPMs, it did not provide a measurement range for classifying the workability of the cold patching materials.

The locking point of the mixtures was measured during compacting them by an SGC. Based on the results, the locking points of the SC, MC, and W*R* at 20 °C were 59, 75, and 51, respectively. Instead, the values recorded at 2 °C were 77, 82, and 49. Considering the SC product as an example, the results indicated that, by reaching 59 gyrations during compaction, the other three gyrations did not change the thickness of the sample and the sample resisted the applied load. Since mixture workability decreases at lower temperatures, the obtained locking points at 2 °C were higher than the locking point at 20 °C. In other words, it takes more energy or many gyrations to compact a poorly workable material. The result of the tests in this study and laboratory observations along with the other research performed by the authors showed that the materials with locking points from 40 to 60 had good to excellent workability. Plus, materials with a locking point higher than 60 were rough and hard to compact. Hemsley also recommends a lock point range of 30–70 for workable cold mixtures [33]. In light of the aforementioned recommended ranges, measuring the locking point of the CMPMs provides adequate information to evaluate their workability.

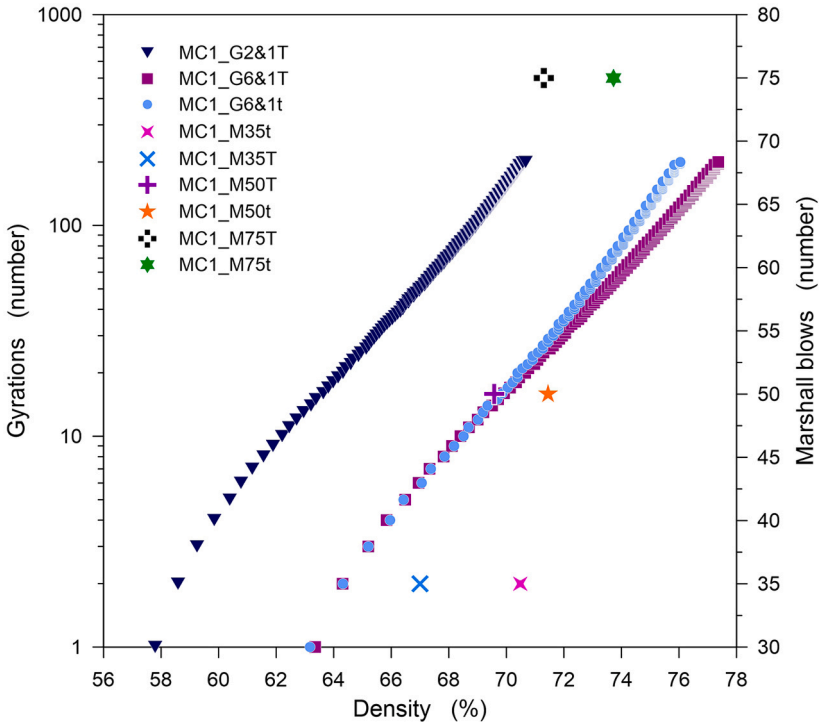

Fig. 6. The density (bulk specific gravity/ theoretical maximum specific gravity) of MC specimens compacted by mixtures SGC or Marshall hammer.

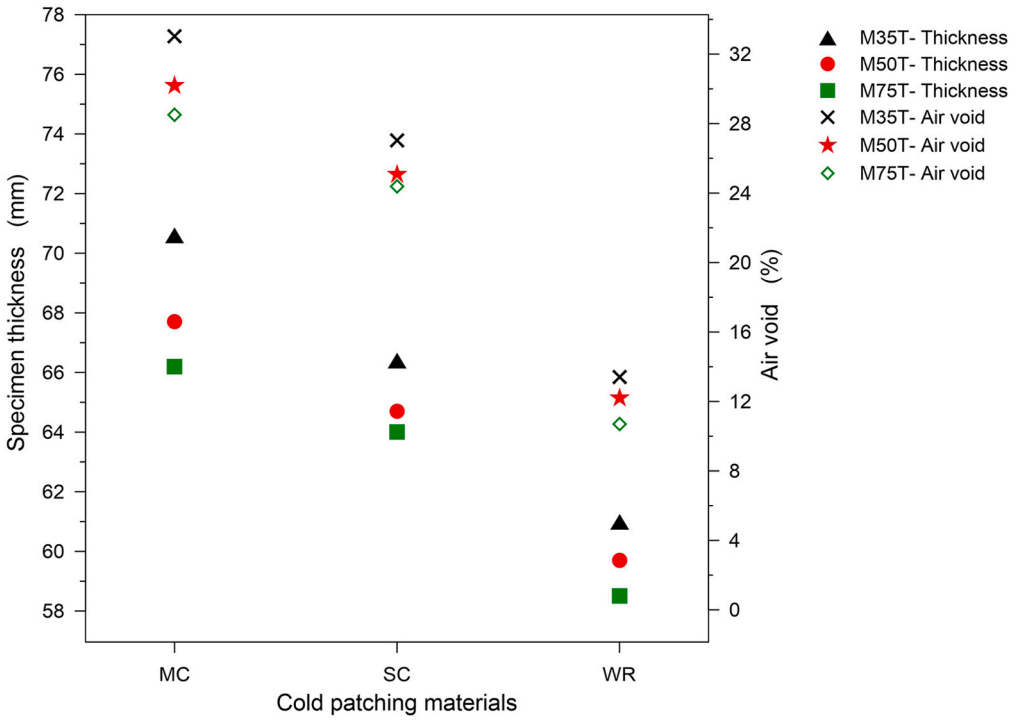

Fig. 7. The thickness and air-void results of CMPMs compacted by the SGC or Marshall hammer.

4.2. Stability

4.2.1. Marshall stability

The Marshall stability values summarized in Table 3 highlight two salient aspects. On the one hand, from a strictly quantitative point of view, the stability measurements for the MC and WR products exceeded the minimum values recommended in the literature for the initial Marshall stability at room temperature and 60 °C, which stand at approximately 2 kN and 0.5 kN, respectively [4]. On the other hand, qualifying the performance of SC mixtures using Marshall stability method was not possible. As, the specimens collapsed during conditioning in 60 °C water. Even at 20 °C the SC briquette specimens were not stable enough at their own weight and started losing adhesion between aggregates and binder (segregation) and collapsed. The stability decreased over time due to insufficient adhesion between the binder and aggregates. Also, higher than 200 kPa pressure was applied to compact the samples, but after a short time, the specimens showed the same results. Thus, it seems that the Marshall stability test method did not cover assessing all types of CMPMs. The test approach failed to determine the initial stability of SC products while the initial stability is crucial for survival of the patch after repair operation. Plus, even poor and low-quality materials such as SC products show some resistance to the traffic load in real condition, however determining the initial stability of these materials was not possible through this method. It is suggested to make thinner specimens to maximize the possibility of their survival after demolding and to acquire considerably more reliable results if the Marshall stability method is employed to assess the performance of CMPMs right after demolding. In the case of an ideal patching operation, stability evaluation would be much more reliable for CMPMs a few weeks after patching (forming stability) rather than immediately. In this case, the specimens are cured long enough (in the mold) to provide sufficient stability after demolding. However, ideal patch placement is barely considered by the repair crew.

Table 3
Marshall stability results of CMPMs.

	Conditioning temperature [°C]					
	20			60		
	Curing time [day]					
	0	7	30	0	7	30
	Marshall Stability [kN]					
SC_G2&1T	1.16	1.88	1.71	*	*	*
MC_G2&1T	2.70	2.82	3.27	0.74	0.80	0.94
WR_G2&1T	7.39	11.33	12.17	1.74	1.75	2.34

* The specimen failed and collapsed before conducting the test.

4.2.2. Indirect tensile strength

The ITS results obtained from the CMPMs (as shown in Table 4) revealed a similar trend to that observed in the Marshall stability test. The results demonstrated that curing time has a substantial effect on the ITS of CMPMs. In the initial stage, all three materials exhibited relatively low ITS values, suggesting that they may not have reached their full-strength potential. However, following the curing period, a significant improvement in ITS values was observed across all materials, signifying a notable enhancement in their tensile strength as the curing process progressed. Longer curing times generally led to increased tensile strength, and the choice of material played a significant role in achieving the final strength. Notably, the W*R* specimens showed significantly higher initial and forming strength compared to the other CMPMs, while the SC specimens demonstrated a decrease in strength seven days after curing. As previously mentioned, the thicker specimens exhibited instability due to inadequate adhesion and stability at their weight, resulting in lower ITS values over time. It is important to note that this test method may not encompass all types of CMPMs, indicating the need for further assessment and development of comprehensive testing approaches. Similar to the results obtained for Marshall stability, the risk of facing strength loss in the first few weeks following the repair operation is not high if the materials are a high-quality product. Therefore, to evaluate the forming strength of the well-compacted patch, a longer curing time and thinner specimens are required to achieve more reliable results.

4.2.3. Hubbard-Field stability

The Hubbard-Field testing approach led to more reliable and reasonable outcomes when evaluating the stability of SC specimens (Table 5). The Hubbard-field thin specimens were more stable at their weights and were much more similar to the field patches and provided fast curing compared to the Marshall briquettes. The findings revealed that determining the initial stability of the SC specimens with Hubbard-Field procedure was possible. However, they were sensitive to the elevated temperature, and the specimens collapsed during conditioning in a water bath at 60 °C. Unlike the Marshall briquettes, which exhibited a decrease in both Marshall stability and ITS values for SC specimens after seven days of curing, the Hubbard-Field stability indicated a rising trend, and the forming stability of all specimens increased even after seven days of curing. It should be emphasized that the results obtained were for specimens that have been compacted for 35 gyrations while in a real condition the densification is higher than the density attained by 35 gyrations in the lab. Therefore, considering a higher number of gyrations than 35 could potentially yield even more reliable results. Except for the possibility of evaluating the stability of the materials, the Hubbard-Field test method provided more functional information about the resistance of the materials to the load and deformation. According to the results presented in Table 5, W*R* materials showed better stability than the other materials, and this fact was also evident in the shape of the tested specimens. The more stable product (Fig. 8-a) showed raised edges after the failure of the specimen. However, for the other poor materials, the specimens' edges were not noticeable (Fig. 8-b). Therefore, despite other stability testing methods like Marshall stability, the Hubbard-Field stability method provided a better view of evaluating the stability of the mixture by analyzing the shape of the examined specimens.

4.2.4. Indentation stability

The evaluation of stability, in terms of depth of indentation, involved the preparations of two different sets of samples, namely mold-surrounded (Fig. 9-a) and mold-free specimens (Fig. 9-b). The first configuration tends to resemble the boundary condition given by the pothole sides. Test analysis of the specimens demonstrated that the mold-surrounded specimens led to more reasonable outcomes than the mold-free ones. The MC and SC mold-free specimens lost their stability less than a few minutes after being subjected to the applied load, in contrast to what happens in in the field when such materials are well compacted and show resistance against the traffic load. The SC specimen showed poor performance and collapsed a few seconds after loading (Fig. 9-b). However, MC materials resisted more and collapsed a few minutes after loading. It seems that the distance between the loading place and the edge of the specimens was not long enough to prevent rapid crack propagation, which led to the failure of the specimens in a short time. Nevertheless, W*R* specimens resulted in the best performance and no evidence of indentation was observed for them even after 24 h.

A time-indentation graph showing the indentation depth over time (1, 2, 4, 8, 15, 30, and 60 min) at 20 °C was plotted to visualize the results of the mold-surrounded specimens (Fig. 10). Indentation of the cylinder into the various specimens increased over time but was not more than 6 mm in one hour. The W*R* specimens, which were very rigid, resisted the static load and did not show any effect of indentation under the load. In other words, the recorded indentation depth was zero for W*R* mix. However, SC and MC products were not as resistant as W*R* materials and showed a maximum of 6 mm of indentation at 60 min. MC specimens showed highest indentation, however, especially at the first 20 min, the slope of the curves on the graph showed that the SC materials have the steeper slope than MC specimens, indicating the specimens had lower stability to withstand the applied load. These results obtained may be affected by the presence of the mold, as crack propagation after loading is restricted by it. As a general suggestion, using larger specimens may

Table 4
ITS results of CMPMs.

Material	Conditioning temperature: 20 °C		
	Curing time [day]		
	0	7	30
	ITS [kPa]		
SC_G2&1T	16.06	26.78	20.46
MC_G2&1T	50.13	58.41	60.56
WR_G2&1T	130.12	256.16	264.53

Table 5
Hubbard-Field stability results of CMPMs.

Material	Conditioning temperature [°C]					
	20			60		
	Curing time [day]					
	0	7	30	0	7	30
	Hubbard-Field stability [kN]					
SC_G2&1t	2.05	2.62	3.19	*	*	*
MC_G2&1t	3.04	3.54	3.91	0.91	1.39	1.73
WR_G2&1t	8.70	12.23	12.54	2.57	5.62	5.93

* The specimen failed and collapsed before conducting the test.

Fig. 8. The Hubbard-Field specimens after conducting the test: a) W*R*; b) MC.

Fig. 9. Tested specimens: (a) mold-surrounded SC specimen (b) mold-free MC specimen.

reduce the impact of rapid crack propagation and mold presence, leading to more reliable results. In addition, the effect of the loading impulse at the beginning of the test should be removed to avoid influencing the results.

4.3. Raveling

The results of mass loss (Table 6), which is considered as an indicator of the raveling resistance showed that the performance of SC mixtures was not satisfactory under different compaction efforts and curing times. The SC specimens immediately showed a high rate of abrasion and raveling and based on the results presented in Table 6, more than 15% mass loss was attained by them during the test. However, the W*R* specimens did not show any noticeable mass loss during the test and the obtained mass loss for this material was almost zero at every condition. Increasing pressure and curing time improved the raveling resistance of W*R* and MC materials. Influence of increasing compaction pressure exceeded curing time, especially in the short time since the weight loss noticeably decreased with increased compaction pressure. For example, the average mass loss of the MC specimens compacted at a pressure of 200 kPa (MC_2&1T) after seven days of curing decreased from 11.65% to 7.26% (a 4.39% percent difference) while increasing the compaction pressure from 200 kPa to 400 kPa resulted in a 2.34% (9.31% percent difference) mass loss. Again, it was noticed that compaction

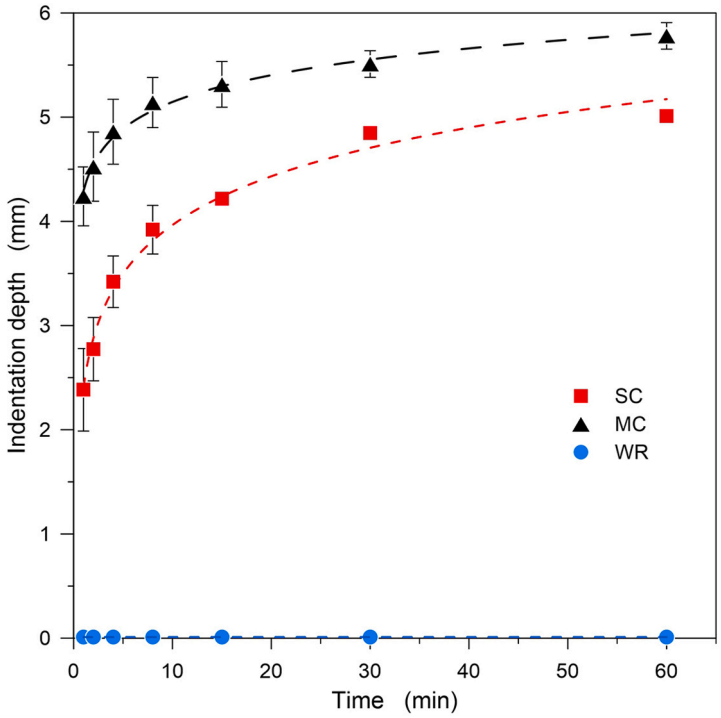

Fig. 10. Indentation test results obtained from mold-surrounded CMPMs at 20 °C.

Table 6
The mass loss percent of CMPMs at different compaction pressures and test time.

		Curing [day]								
		0			7			30		
		Test time [s]								
		30	60	120	30	60	120	30	60	120
		Mass loss [%]								
MC	2&1T	11.65	*	*	7.26	*	*	4.89	10.92	11.91
	4&1T	2.34	3.63	4.00	0.92	7.26	*	*	4.89	10.92
	6&1T	0.64	1.32	1.61	0.27	0.92	1.30	2.13	0.66	1.15
SC	2&1T	*	*	*	*	*	*	*	*	*
	4&1T	*	*	*	*	*	*	12.80	*	*
	6&1T	*	*	*	*	*	*	*	*	*
WR	2&1T	0.22	0.36	0.59	0.00	0.00	0.00	0.00	0.00	0.00
	4&1T	0.00	0.00	0.00	0.00	0.00	0.00	0.00	0.00	0.00
	6&1T	0.00	0.00	0.00	0.00	0.00	0.00	0.00	0.00	0.00

*The test failed, and the specimens led to higher rate of abrasion (mass loss> 15%).

pressure and densification were crucial for enhancing patch durability. Nevertheless, if the compaction pressure is too high, it can lead to worse abrasion results. Applying a compaction pressure of 600 kPa to SC mixes (SC_6&1T) resulted in aggregate breakage and, subsequently, a higher abrasion rate. Therefore, the mix design and the quality of the mixture components should be considered when applying higher energy to compact the material. Furthermore, since the raveling of the patch starts immediately after the repair operation and the compaction effect is higher than the curing time, evaluating the raveling by brush test after making the specimens can provide a better view of the performance of the patch. If the patch survives after filling the pothole, the curing and the associated traffic compaction will improve the patch's resistance to raveling. In addition, the wide range of motion of the wire brush (with an external diameter of 60 mm) on the specimens (with a diameter of 102 mm) increased the stress concentration at the specimen edges, which led to rapid and premature failure of the specimen. Considering larger specimens (with a diameter of 150 mm) can provide a wider surface for the wire brush movements and prevent the stress concentration at the edges, leading to more reliable results.

4.4. Bonding

Bonding, which refers to the amount of energy required to break the adhesion between two layers, was determined for the patching material and the reference layer and the results were presented in Table 7. The numerical values of the parameters showed that the W*R* materials led to better bonding performance against the applied shear load compared to the other materials. Although W*R* specimens absorbed a higher amount of energy before starting to fail, they showed higher stiffness and brittleness compared to the others, as the initial slope and the sharply dropping post-peak curve observed for W*R* specimens were steeper than those observed for MC and SC specimens (Fig. 11). Also, SC materials that showed poor performance in other evaluation tests led to a better interface bond compared to the MC. According to Table 7 and graphs of Fig. 11, the SC specimens exhibited significantly greater energy requirements in terms of pre-peak, post-peak, and total energy for detaching from the underlying HMA layer compared to the MC specimens. These findings highlighted that the SC specimens possess enhanced adhesive characteristics and higher resistance to shear forces, thereby forming a stronger and longer-lasting bond. Consequently, it necessitated a higher amount of energy to counteract this adhesive strength and induce failure in the specimens. Debonding of the patch can happen immediately after a repair operation and reopening to traffic, leading to the premature failure of the patch. Although the compaction and curing of the materials improve the bonding between the patch and the old pavement, time and a higher compaction effort are required to see their effect on the interface bond. Therefore, assessing the material bonding properties after patch operation is recommended to prevent premature failure of the patches.

5. Conclusion

In this study, a comprehensive range of laboratory tests and innovative adaptations to existing ones, such as Marshall stability, indirect tensile strength (ITS), Hubbard-Field stability, indentation stability, Leutner shear bond, locking point, and brush tests, were proposed for the evaluation of the properties and performance of cold mix patching materials (CMPMs). To assess the effectiveness of these tests on CMPMs, three different types of patch materials, representing the primary categories of CMPMs currently available in the market, were investigated. The specimens were prepared using a Superpave gyratory compactor (SGC) and Marshall hammer, with compaction pressures ranging from 200 to 600 kPa and 35–75 blows. The key findings can be summarized as follows:

- The qualification of a CMPM and the expression of the expected performance results in the field cannot be separated from a preliminary laboratory characterization that examines the designed properties, from workability to the achievement of proper strength levels reached at different temperatures, and from opening to traffic to longer times (weeks, months). Thus, it is necessary to link the CMPM to performance-related indicators referred to critical times, temperatures and stress conditions and calculated at those specific times and temperatures. The authors demonstrated how existing test methods used for HMAs can be usefully adapted to explore the peculiar characteristics of CMPMs.
- Compaction is perhaps the most significant, in actual fact essential, parameter. Significant compaction pressure is necessary to replicate the field compaction in the laboratory to prepare cylindrical specimens: the air-void (density) contents obtained from the field patches closely matched the values obtained from laboratory specimens, whether they were thick ($t = 65 \pm 5$ mm) or thin ($t = 35 \pm 5$ mm), and subjected to 75 Marshall hammer blows or 600 kPa for 200 gyrations in the Superpave gyratory compactor (SGC). However, when dealing with deeper potholes or aiming to simulate thicker patches, the SGC proved to be more effective than the Marshall hammer in replicating field patch compaction in the laboratory.
- Using the locking point of the CMPMs to evaluate their workability presented a viable range for assessing the workability of the mixtures. Materials exhibiting locking points between 40 and 60 demonstrated good to excellent workability, while those with locking points exceeding 60 proved to be challenging and resistant to compaction.
- Employing Marshall stability and ITS tests for unaged specimens provided more accurate results, but these methods did not cover the full range of CMPM types and curing times. Shorter specimens are recommended for immediate post-demolding evaluation to prevent specimen collapse.
- The Hubbard-Field test method facilitated a thorough assessment of various CMPMs, particularly those facing performance challenges, delivering precise and coherent results in contrast to conventional methods such as Marshall stability and ITS. Notably, in this test, stable specimens displayed raised edges upon failure, serving as a distinct indicator of their superior performance. Similarly, the Indentation stability test, enabled the assessment of the stability of underperforming mixtures, offering also the advantage to better simulates the boundary conditions presented by pothole sides in the real-world conditions.

Table 7
Bonding results of the selected CMPMs.

Material		$F_{SBT,max}$ [kN]	F'_{SBT} [kN/mm]	$\tau_{SBT,max}$ [kPa]	$K_{SBT,max}$ [Pa/mm]	Eng_A [N•mm]	Eng_B [N•mm]
SC	Average	0.41	0.40	50.11	48.42	283.96	367.59
	ST. DEV.	0.03	0.01	3.55	0.75	63.80	78.52
MC	Average	0.34	0.58	41.98	71.05	85.74	127.30
	ST. DEV.	0.05	0.20	6.26	24.11	21.75	35.06
W*R*	Average	1.55	2.54	189.32	310.32	673.46	566.68
	ST. DEV.	0.12	0.05	14.71	6.18	63.10	42.37

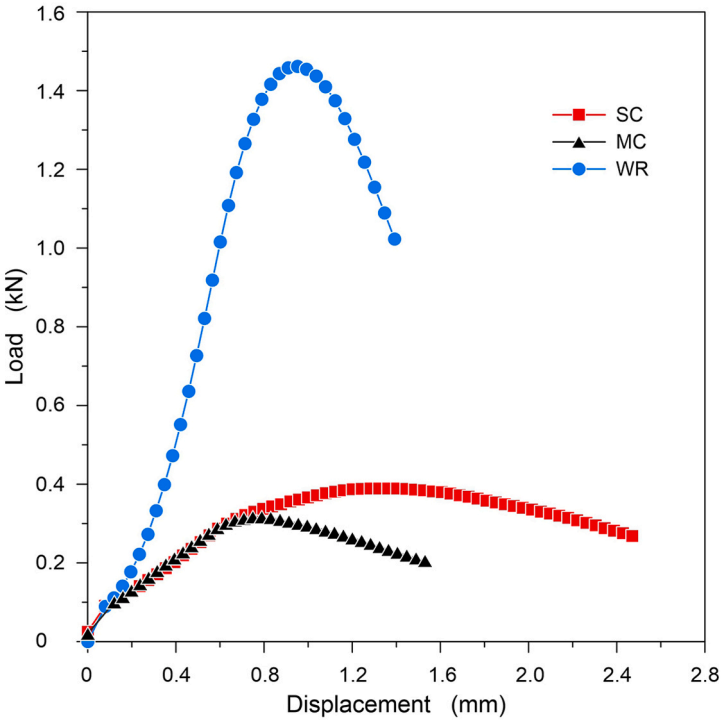

Fig. 11. The shear force vs. the displacement obtained from the shear bond test at 20 °C.

- The Brush test simulated tire rotation and mechanical dislodging more effectively than the currently used Cantabro test. However, it revealed stress concentration issues at specimen edges. To enhance reliability, using larger 150 mm diameter specimens is suggested. During the test, SC mixtures displayed poor raveling resistance with over 15% mass loss, whereas WR mixtures showed no significant mass loss.
- Unlike alternative tests, the Leuthner shear bond test excelled at replicating real-world conditions with ease. In contrast to the SC's underperformance in other tests, it exhibited superior bonding properties compared to the MC material.

The outcomes of this study offer CMPM designers and material users valuable insights into the performance of CMPMs under various weather and traffic conditions, enabling manufacturers to enhance their product characteristics through diverse testing approaches. Furthermore, this study paves the way for researchers to explore different aspects of CMPMs' performances and encourages them to improve test methods for analyzing and evaluating patching materials. As the market penetration of CMPMs in the field of rapid road maintenance solutions continues to experience significant growth, these findings hold particular importance.

Declaration of Competing Interest

The authors declare that they have no known competing financial interests or personal relationships that could have appeared to influence the work reported in this paper.

Data Availability

Data will be made available on request.

Acknowledgement

Some activities were partially funded under the National Recovery and Resilience Plan (NRRP), Mission 4 Component 2 Investment 1.5 - Call for tender No. 3277 of 30/12/2021 of Italian Ministry of University and Research funded by the European Union – NextGenerationEU, Project code ECS00000033, CUP D93C22000460001, "Ecosystem for Sustainable Transition in Emilia-Romagna."

References

[1] A. Abdukadir, Z. Pei, W. Yu, J. Wang, A. Chen, K. Tang, J. Yi, Performance optimization of epoxy resin-based modified liquid asphalt mixtures, Case Stud. Constr. Mater. 17 (2022), e01598, https://doi.org/10.1016/j.cscm.2022.e01598.

[2] Z. Sun, Y. Ma, S. Liu, Y. Li, X. Qiu, Z. Luo, Evaluation of engineering properties of Fiber-reinforced Usual-temperature Synthetic Pitch (USP) modified cold mix patching asphalt, Case Stud. Constr. Mater. 16 (2022), e00997, https://doi.org/10.1016/j.cscm.2022.e00997.
[3] L. Geng, Q. Xu, X. Yu, C. Jiang, Z. Zhang, C. Li, Laboratory performance evaluation of a cold patching asphalt material containing cooking waste oil, Constr. Build. Mater. 246 (2020), 117637, https://doi.org/10.1016/j.conbuildmat.2019.117637.
[4] L.D. Zhao, Y.Q. Tan, A summary of cold patch material for asphalt pavements, Advanced Materials Research, Trans. Tech. Publ. (2011) 864–869, https://doi.org/10.4028/www.scientific.net/AMR.168-170.864.
[5] K. Orhan, Experimental investigation of usability of 100% recycled asphalt pavement (RAP) as a cold patching material in Turkey, Karadeniz Fen. Bilim. Derg. 13 (1) (2023) 223–231, https://doi.org/10.31466/kfbd.1230440.
[6] M. Pasetto, G. Giacomello, E. Pasquini, A. Baliello, Recycling bituminous shingles in cold mix asphalt for highperformance patching repair of road pavements, Pavement Asset Manag. (2019) 627–634, https://doi.org/10.1201/9780429264702-75.
[7] R. Hafezzadeh, F. Autelitano, F. Giuliani, The effect of using flux oil and RAP on the performance of pavement cold mix patching materials, Transp. Res. Procedia 69 (2023) 616–622, https://doi.org/10.1016/j.trpro.2023.02.215.
[8] M. Isabela, R. Spielhofer, Rapid and durable maintenance methods and techniques, Final report, ERA-NET Road – Design, Austria, 2014.
[9] Department for Transport. Prevention and a better cure: potholes review, UK DfT, London, 2012.
[10] S. Chatterjee, R.P. White, A. Smit, J. Prozzi, J.A. Prozzi, Development of mix design and testing procedures for cold patching mixtures, Report No. FHWA/TX-05/0–4872-1, Federal Highway Administration, Texas Department of Transportation, Austin, Texas, 2006.
[11] X. Huang, J. Luo, P. Tang, C. Xie, J. Chen, Preparation and study of a pu-modified epoxy resin cold patching mixture, 175–180-175–180, Mater. Technol. 57 (2) (2023), https://doi.org/10.17222/mit.2023.748.
[12] M.D. Nazzal, S.-S. Kim, A.R. Abbas, Evaluation of winter pothole patching methods, Report No. FHWA/OH-2014/2, Ohio. Dept. of Transportation. Office of Statewide Planning and Research, 2014.
[13] M.-C. Liao, C.-C. Luo, T.-Y. Wang, X. Xie, Developing effective test methods for evaluating cold-mix asphalt patching materials, J. Mater. Civ. Eng. 28 (10) (2016), 04016108, https://doi.org/10.1061/(ASCE)MT.1943-5533.0001639.
[14] G. Cerni, A. Corradini, Compaction characteristics assessment of cold mix patching materials through gyratory shear compactor, Constr. Build. Mater. 364 (2023), 129926, https://doi.org/10.1016/j.conbuildmat.2022.129926.
[15] R. Hafezzadeh, F. Autelitano, F. Giuliani, Asphalt-based cold patches for repairing road potholes–An overview, Constr. Build. Mater. 306 (2021), 124870, https://doi.org/10.1016/j.conbuildmat.2021.124870.
[16] M. Rezaei, L. Hashemian, A. Bayat, B. Huculak, Investigation of rutting resistance and moisture damage of cold asphalt mixes, J. Mater. Civ. Eng. 29 (10) (2017), 04017193, https://doi.org/10.1061/(ASCE)MT.1943-5533.0002042.
[17] P.S. Kandhal, D.B. Mellott, Rational approach to design of bituminous stockpile patching mixtures, Transp. Res. Rec. 821 (1981) 16–22.
[18] T.P. Wilson, A.R. Romine, Innovative materials development and testing. Volume 2: Pothole repair, Report No. SHRP-H-353, Strategic Highway Research Program, Washington, D.C., 1993.
[19] A. Maher, N. Gucunski, W. Yanko, F. Petsi, Evaluation of pothole patching materials, Report no. FHWA 2001–02, Washington, D.C., U.S.A., 2001.
[20] C.K. Estakhri, J.W. Button, Test methods for evaluation of cold-applied bituminous patching mixtures, Transp. Res. Rec. 1590 (1) (1997) 10–16, https://doi.org/10.3141/1590-02.
[21] Y. Bi, R. Li, S. Han, J. Pei, J. Zhang, Development and performance evaluation of cold-patching materials using waterborne epoxy-emulsified asphalt mixtures, Materials 13 (5) (2020) 1224, https://doi.org/10.3390/ma13051224.
[22] Y. Cheng, X. Zhang, Y. Dong, J. Chen, Preparation and road performance of solvent-based cold patch asphalt mixture, Int. J. Pavement Res. Technol. 15 (2022) 1155–1165, https://doi.org/10.1007/s42947-021-00079-1.
[23] J.E. Shoenberger, W.D. Hodo, C.A. Weiss Jr, P.G. Malone, T.S. Poole, Expedient repair materials for roadway pavements, Engineer Research & Development Center Vicksburg MS Geotechnical and Structures Laboratory, 2005.
[24] H.P. Wang, R. Zhang, Z.Y. He, J.Z. Wang, Deformation behaviors of dilution type cold patch asphalt mixture under different stress modes, Appl. Mech. Mater. Trans. (2017) 114–118, https://doi.org/10.4028/www.scientific.net/AMM.872.114.
[25] D. Ghosh, M. Turos, M. Marasteanu, Experimental investigation of pothole repair materials, Proceedings of the 9th International Conference on Maintenance and Rehabilitation of Pavements—Mairepav9, Springer, 2020, pp. 13–22. https://doi.org/10.1007/978–3-030–48679-2_2.
[26] D. Anderson, H. Thomas, Z. Siddiqui, D. Krivohlavek, More effective cold, wet weather patching materials for asphalt pavements, Report No. FHWA-RD-88–00l, Federal Highway Administration, Pennsylvania Transportation Institute, 1988.
[27] S. Biswas, L. Hashemian, M. Hasanuzzaman, A. Bayat, A study on pothole repair in Canada through questionnaire survey and laboratory evaluation of patching materials, Can. J. Civ. Eng. 43 (5) (2016) 443–450, https://doi.org/10.1139/cjce-2015-0553.
[28] B.D. Prowell, A.G. Franklin, Evaluation of cold mixes for winter pothole repair, Transp. Res. Rec. 1529 (1) (1996) 76–85, https://doi.org/10.1177/0361198196152900110.
[29] V. Rosales, J. Prozzi, J. Prozzi, Mixture design and performance-based specifications for cold patching mixtures, Report No. FHWA/TX-08/0–4872-2, The University of Texas at Austin, Center for Transportation Research, 2007.
[30] X. Wang, Y. Huang, L. Geng, M. Li, H. Han, K. Li, Q. Xu, Y. Ding, T. Zhang, Multiscale performance of composite modified cold patch asphalt mixture for pothole repair, Constr. Build. Mater. 371 (2023), 130729, https://doi.org/10.1016/j.conbuildmat.2023.130729.
[31] M. McHale, C. Nicholls, I. Carswell, Best practice guide for the selection of pothole repair options, Report No. RN44, Transport Research Laboratory, 2016.
[32] M.J. Rogers, H.A. Wallace, Design and Construction of Asphalt Pavements, McGraw-Hill, 1957.
[33] C. Ling, H.U. Bahia, Development of a volumetric mix design protocol for dense-graded cold mix asphalt, J. Transp. Eng. Part B: Pavements 144 (4) (2018) 04018039, https://doi.org/10.1061/JPEODX.0000071.